Appl. Magn. Reson. 29, 159–169 (2005)

Applied Magnetic Resonance

A Localization Method for the Measurement of Fast Relaxing ^{13}C NMR Signals in Humans at High Magnetic Fields

G. Öz, P.-G. Henry, I. Tkáč, and **R. Gruetter**

Center for Magnetic Resonance Research, University of Minnesota, Minneapolis, Minnesota, USA

Received July 22, 2004; revised October 29, 2004

Abstract. Nuclear magnetic resonance (NMR) signals with short T_1 and T_2, such as the ^{13}C signal of glycogen, are difficult to localize in three dimensions without major signal loss. A pulse sequence that accomplishes the spatial localization of ^{1}H-decoupled ^{13}C NMR signals on a whole-body scanner within the Food and Drug Administration guidelines for specific absorption rates was designed. The method uses an optimized three-dimensional outer volume suppression scheme combined with one-dimensional image-selected in vivo spectroscopy and surface coil detection. The localization performance of the sequence was validated at 4 T with double chambered phantoms and ^{13}C magnetic resonance imaging. Localized ^{13}C spectra were acquired from human brain and muscle.

1 Introduction

In vivo ^{13}C nuclear magnetic resonance (NMR) spectroscopy is a powerful method to study dynamic biological processes. After infusing ^{13}C-labeled compounds, the time courses of label incorporation into metabolites above the 1.1% natural abundance can be measured in humans and animals. Such studies yield estimates of metabolic fluxes and aid in understanding of carbohydrate and lipid metabolism [1–3]. To harness the potential of such measurements, quantification and spatial localization in a well-defined area are important. For example, a reliable measurement of compounds in the brain requires suppression of signals from the extracerebral muscle and fat tissue.

In vivo ^{13}C NMR is currently the only noninvasive method capable of quantifying glycogen in human tissues [1, 4]. However, NMR studies of glycogen metabolism have been performed without three-dimensional (3-D) localization due to challenges brought about by its very short T_1 (about 150–160 ms at 4.7 T) and T_2 (about 5–10 ms at 4.7 T) relaxation times [5, 6]. The development of a localization method to study such biologically important, large molecules in humans is of great interest. Methods that perform localization on transverse magnetization (echo-based methods) can be used for the spatial localization of mol-

ecules with sufficiently long T_2; however, they suffer from signal loss when T_2 is short. A commonly utilized localization method that does not depend on echo formation, 3-D image-selected in vivo spectroscopy (ISIS) [7], inverts the magnetization in a slice, selected by the use of field gradients, every other scan. The signal from the slice of interest is then obtained by subtraction of the inverted from the noninverted scans, leading to an add-subtract scheme of 8 acquisitions that contain up to three 180° pulses. However, 3-D ISIS is not applicable to the study of compounds with short T_1, due to relaxation during the time between the first inversion pulse and excitation. Therefore a nonecho localization method that minimally manipulates the magnetization in the volume of interest (VOI) is preferable for the localization of compounds with very short relaxation times. Such a method based on outer volume suppression (OVS) has been described [8] and used to measure in vivo glycogen metabolism in the rat brain [9] and mouse liver [10].

In order to apply a similar localization technique to the human brain, however, specific absorption rate (SAR) limits set forth by the Food and Drug Administration (FDA) need to be observed to avoid tissue heating. The SAR limits represent a major obstacle to localization of ^{13}C signals in humans because of the necessity to decouple the protons bound to carbons and the substantially higher radio-frequency (RF) power requirements to achieve large bandwidths due to the low gyromagnetic ratio of ^{13}C. Additionally, the T_1 relaxation time of glycogen at a high-field (4 T) whole-body scanner is shorter than its T_1 at the magnetic field utilized for the rodent measurements (9.4 T) [8] making fast repetition rates necessary for optimal signal-to-noise ratios (SNR). In order to repeat the pulse sequence reasonably fast without exceeding the SAR limits, the localization method for fast-relaxing compounds in the human needs to utilize the minimum number of pulses that will acceptably suppress the signal from outside the VOI.

The aim of the current study was to develop an OVS-based 3-D localization method that can be applied to humans at 4 T within the SAR limits, including those set for the brain.

2 Materials and Methods

2.1 Instrumentation

All measurements were performed on a 4 T, 90 cm bore magnet (Oxford Magnet Technology, Oxford, UK) with an INOVA console (Varian, Palo Alto, CA). A quadrature 14 cm ^{1}H surface coil combined with a 9 cm diameter linearly polarized ^{13}C coil was used [11]. Prior to the ^{13}C NMR measurements, the following adjustments were performed. After tuning the coil, axial magnetic resonance imaging was acquired using a multislice RARE (rapid acquisition relaxation-enhanced) sequence (repetition time [TR], 4 s; echo train length, 8; echo time, 60 ms; 7 slices) to determine the voxel position for spectroscopy. All first- and second-order shims were adjusted by FASTMAP with echo-planar readout [12]. RF power requirements were calibrated in phantoms relative to the signal from a small sphere containing 99% enriched ^{13}C formic acid placed at the ^{13}C

coil center. The power deposition was measured at the coil port. These values were multiplied by the power factors of the pulses and coil efficiency (83%) to calculate average SAR, assuming most of the power will be absorbed by 1.5 kg of tissue [11]. With the use of a surface coil, the local SAR is highest at the tissue surface. Therefore, an upper limit for the local SAR was calculated for the first centimeter of tissue on the basis of previous estimates [11]. Namely, the volume of the first centimeter of tissue is at least 160 ml and at most 21% of the total irradiated power is deposited within this slice. Both average and local SAR values were within the FDA guidelines (<3 W/kg average, 8 W/kg local for head measurements). This was consistent with over 8 years of continuous experience of using this RF coil technology [11, 13–19].

2.2 Pulse Sequence

The pulse sequence for 3-D localization consisted of two parts (Fig. 1). First, OVS was applied in three dimensions. This was achieved by applying double-banded broadband hyperbolic secant pulses (8 ms, 22 kHz bandwidth) as nominal 90° pulses in slices on two sides of the VOI along x and z (for designations of the dimensions see Fig. 2). The transverse magnetization was then dephased by the rampup periods (2 ms) of the slice selection gradients of the next dimension. This approach reduced the acoustic noise generated by the gradients. Similarly, the slice between the RF coil and the VOI was dephased after selection with a hyperbolic secant pulse (6 ms, 42 kHz bandwidth). Next, signal selection in the slice parallel to the ^{13}C coil (y-slice) was improved by applying a 180° hyperbolic secant pulse (4 ms, 22 kHz bandwidth) on alternate

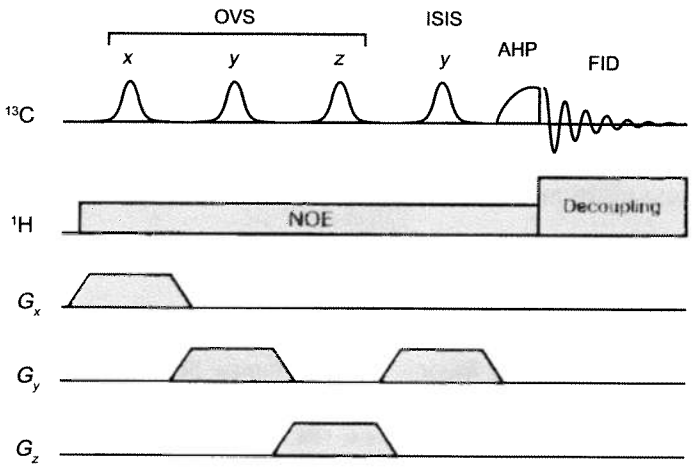

Fig. 1. Pulse sequence diagram for 3-D localization of fast-relaxing ^{13}C signals. OVS pulses are applied in three dimensions, followed by ISIS in one dimension. AHP, adiabatic half passage; FID, free induction decay; NOE, nuclear Overhauser effect.

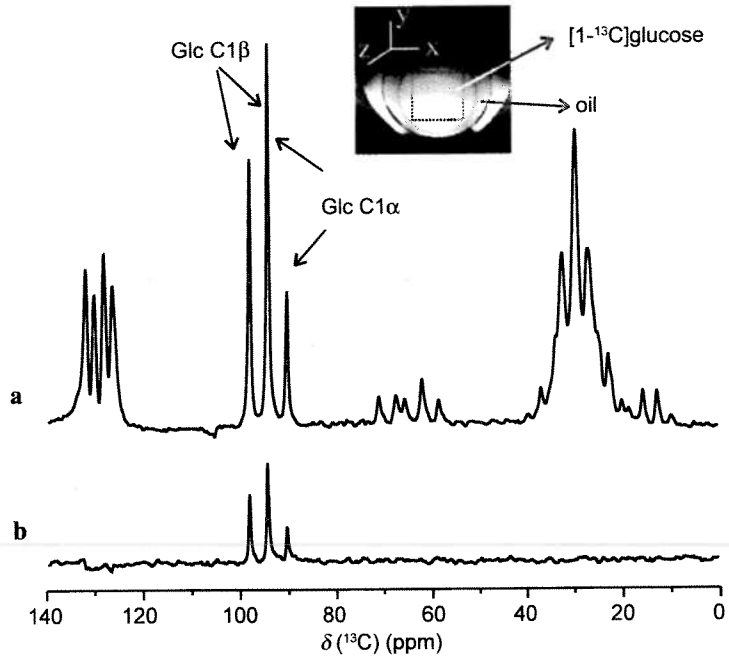

Fig. 2. Proton-coupled ^{13}C NMR spectra of a two-compartment phantom containing [1-^{13}C]glucose (inner compartment) and natural-abundance vegetable oil (outer compartment) without (**a**) and with (**b**) localization (16 transients, TR = 6 s). The C-1 signals of the α and β forms of glucose are marked. The remaining resonances originate from lipids. The VOI (6 by 6 by 6 cm) is shown on the transverse T_2-weighted image (inset). Saline bags were placed outside the phantom to increase the loading of the coil.

scans amounting to 1-D ISIS localization [7] immediately before the excitation pulse. The total time required for localization was 35 ms. Excitation was achieved with a 2 ms adiabatic half-passage pulse. Bi-level WALTZ-16 [20] was used for NOE generation during the relaxation delay and for decoupling during acquisition ($\gamma B_2/2\pi$ was 16 Hz for NOE and 400 Hz for decoupling at coil center). Decoupling contributed 50% to the total SAR deposited (at an acquisition time of 25 ms), the x and z OVS pulses 29% and y-slice ISIS 14%.

2.3 In Vivo Studies

Healthy volunteers were studied after giving informed consent using procedures approved by the Institutional Review Board: Human Subjects Committee. Subjects were positioned supine on the patient bed with the occipital lobe above the surface coil for the brain studies and the calf muscle for the muscle measurements. They wore earplugs to minimize gradient noise and were positioned in the coil holder with cushions to minimize movement.

In order to detect human brain glycogen, ^{13}C-labeled glucose was administered to one subject. Intravenous catheters placed antegrade in contralateral arms

were used for glucose infusion and blood sampling. A total of 450 g of [1-^{13}C]-glucose (prepared as 20% weight-to-volume D-glucose in water with 99% isotopic enrichment) was administered into the arm vein over 22 h and the [^{13}C]glycogen signal followed in the occipital lobe for 55 h from the start of infusion. The isotopic enrichment of the plasma glucose was measured by gas-chromatography–mass spectroscopy (GC-MS) and was 80% on average during the infusion.

Quantitation of the ^{13}C label in the C-1 position of glycogen was done by the external referencing method as described previously [19]. A phantom that contained 450 mM natural-abundance oyster glycogen was prewarmed and spectra were acquired from the same voxel position with identical acquisition parameters as in vivo. The following equation that takes into account the 1.1% natural abundance of ^{13}C in the phantom was used to calculate the label concentration in brain glycogen:

$$[^{13}\text{C glycogen}] = \frac{I_{\text{Glyc}}(\text{brain}) \cdot I_{\text{FA}}(\text{phantom}) \cdot 450\ \text{mM} \cdot 0.011}{I_{\text{FA}}(\text{brain}) \cdot I_{\text{Glyc}}(\text{phantom})}, \quad (1)$$

where I denotes integrated signal intensity, and the subscripts Glyc for glycogen and FA for formic acid. Determination of peak areas was accomplished with the built-in spectrometer software. Concentrations were converted to micromole per gram on the basis of a specific density of brain tissue of approximately 1 g/ml. The normalization of the glycogen integral to the formic acid signal was applied to correct for small differences in coil loading in vivo and in vitro (about 2 dB).

2.4 Chemicals

D-[1-^{13}C]glucose (99% enriched) was purchased from Isotec Inc, Miamisburg, OH, oyster glycogen from Sigma, St. Louis, MO, and ethylene glycol (>95%) from Fisher Scientific, Pittsburgh, PA.

3 Results

3.1 Validation of the Localization Performance of the Sequence

Unlocalized in vivo ^{13}C spectra of the human head contain large extracerebral lipid signals, while normal human brain does not contain detectable triacylglycerol resonances [13]. The suppression of these extracerebral lipid signals validates efficient localization within the brain. Therefore, a double-chambered phantom, the outer compartment of which mimicked the lipid layer outside the brain, was utilized to test the localization performance of the pulse sequence (Fig. 2). The phantom contained commercially available vegetable oil in the outer compartment (3 liters) and 40 mM [1-^{13}C]glucose in the inner compartment (1 liter). Upon application of the localization sequence all of the lipid signals were suppressed to the noise level (Fig. 2).

The localization of compounds with very short T_1 and T_2 was tested in a phantom that contained 450 mM of natural-abundance oyster glycogen (5 mM [^{13}C]gly-

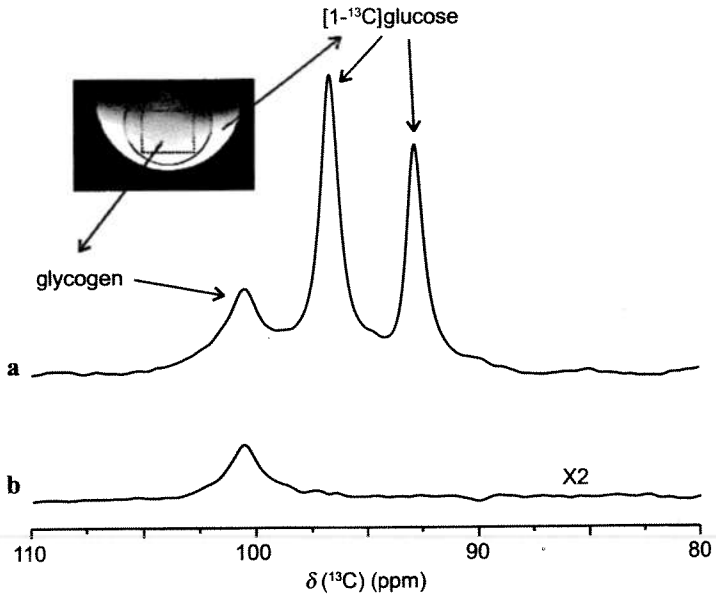

Fig. 3. Proton-decoupled ^{13}C NMR spectra of a two-compartment phantom containing natural-abundance glycogen (inner compartment) and [1-^{13}C]glucose (outer compartment) without (**a**) and with (**b**) localization (256 transients were acquired for the unlocalized, 2048 transients for the localized spectrum, TR = 1 s). The VOI (6 by 5 by 6 cm) is shown on the transverse T_2-weighted image (inset). The C-1 peaks of glycogen and glucose are marked. The spectra were line-broadened by 30 Hz.

cogen) in the inner compartment (1 liter) and 10 mM [1-^{13}C]glucose in the outer compartment (3 liters). The localization sequence suppressed the glucose signal originating from the outer compartment to noise level (Fig. 3). A TR of 1 s was selected to reduce suppression of the glucose signal due to saturation. The optimal TR for glycogen localization in vivo is shorter than this value (see below).

Finally, to visualize the localization performance of the sequence, ^{13}C images were acquired with a gradient echo sequence following the localization sequence (Fig. 4). To achieve high ^{13}C signal intensity, a phantom containing natural-abun-

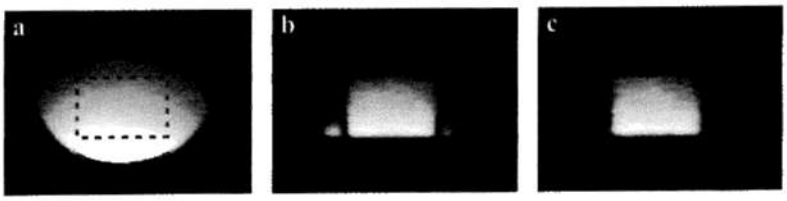

Fig. 4. ^{13}C MRI of the efficiency of the localization method. The transverse image of ethylene glycol was acquired with a gradient-echo sequence (TE = 7.4 ms, TR = 0.5 s, 128 phase encoding steps). **a** ^{13}C image without localization, **b** after localization with the sequence described in Fig. 1, **c** after localization with a low-power OVS pulse in x dimension added to the beginning of the sequence described in Fig. 1. The localized volume (7 by 5 by 6 cm) is shown with a dashed line in **a**.

dance ethylene glycol was utilized. The slice parallel to the RF coil (y-slice) was selected with no detectable contamination from outside the VOI along y. The localized image contained little signal from outside the VOI in the x and z dimensions in areas close to the surface coil (Fig. 4b). This signal had an opposite phase relative to the signal from the VOI and therefore was likely caused by the magnetization experiencing higher than a 90° OVS pulse due to the B_1 inhomogeneity of the surface coil. The signal from outside the VOI was eliminated by adding to the beginning of the sequence another OVS pulse in the x dimension to excite a narrow band (2.5 cm) outside the VOI with approximately one-third of the power of the main OVS pulse in the x dimension (Fig. 4c). Addition of low-power pulses in both the x and z dimensions increased the SAR by 8% and the sequence could still be executed with in vivo power requirements at TR of 0.3–0.45 s within the SAR limit for the brain (3 W/kg).

3.2 In Vivo Studies

Localized ^{13}C spectra were acquired from the human brain with the present method and natural-abundance signals from high-concentration metabolites, in particular *myo*-inositol, were detected (Fig. 5). The localization sequence suppressed the lipid (glycerol) signals from the scalp at 62 and 69 ppm to the noise level which made it possible to detect the weak metabolite signals.

The performance of the sequence with fast-relaxing signals was first tested by acquisition of glycogen spectra in the human calf muscle. The concentration

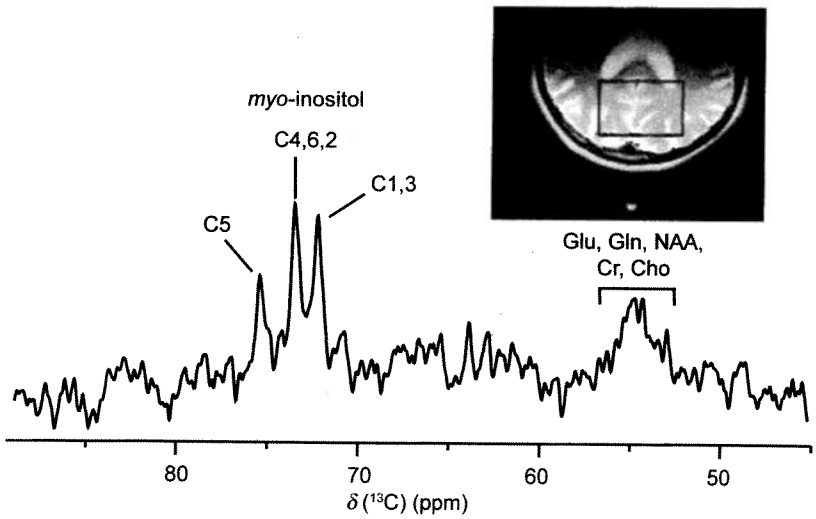

Fig. 5. Proton-decoupled localized natural-abundance ^{13}C NMR spectrum of *myo*-inositol in the human brain (800 transients, TR = 3 s). The VOI (6 by 4 by 6 cm) is shown on the transverse T_2-weighted image (inset). The resonances originating from the different carbons of *myo*-inositol are marked. Glu, glutamate; Gln, glutamine; NAA, N-acetyl-aspartate; Cr, creatine; Cho, choline.

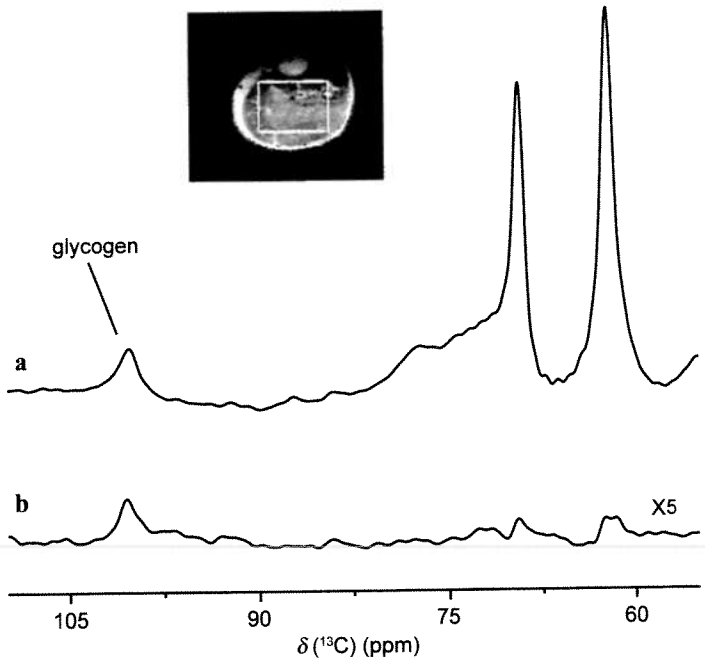

Fig. 6. Proton-decoupled natural-abundance ^{13}C NMR spectrum of glycogen in the human calf muscle without (**a**) and with (**b**) localization (640 transients were acquired for the unlocalized, 6400 transients for the localized spectrum, TR = 0.3 s). The VOI (7 by 5 by 6 cm) is shown on the transverse T_2-weighted image (inset). The C-1 peak of glycogen at 100.5 ppm is marked. The peaks at 62 and 69 ppm in **a** originate from glycerol in triacylglycerides.

of glycogen in the muscle is high (50–100 mM) allowing the detection of its natural-abundance signal [21]. However, unlocalized muscle ^{13}C spectra also contain a large lipid signal that primarily originates from subcutaneous fat tissue and introduces baseline artifacts when weaker signals such as glycogen are studied (Fig. 6a). The application of the localization sequence to the human leg suppressed this lipid signal and allowed detection of the muscle glycogen without baseline complications (Fig. 6b).

Brain glycogen, on the other hand, is only detectable after labeling it with [^{13}C]glucose due to its low concentration [19]. An example of brain glycogen detection in the occipital lobe and quantitation of its signal is demonstrated in Fig. 7. Label incorporation into brain glycogen from [1-^{13}C]glucose, followed by the label wash-out, was measured over 55 h with the described localization technique.

4 Discussion

Here we report the development of a 3-D localization technique for ^{13}C NMR spectroscopy in humans of compounds with very short T_1 and T_2 relaxation times. With double-chambered phantoms we showed that the signal from outside the

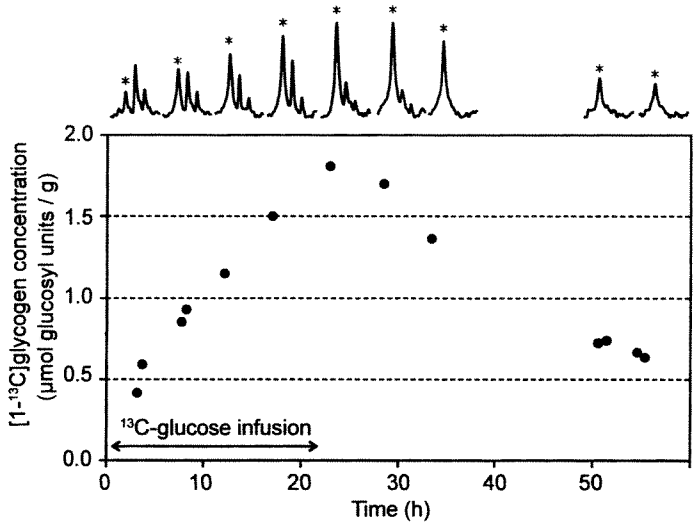

Fig. 7. Label incorporation from [1-^{13}C]glucose into and washout from brain glycogen in one subject. Proton-decoupled ^{13}C NMR spectra are shown at the corresponding time points. The C-1 peak of glycogen at 100.5 ppm is marked with an asterisk, the other 2 peaks are α and β C-1 glucose. Each data point and spectrum represent 5120 transients, TR = 0.3 s. The VOI was 7 by 5 by 6 cm in the ocipital lobe.

VOI was suppressed to the noise level upon application of the localization method (Figs. 2 and 3). We acquired localized ^{13}C spectra in humans and detected natural-abundance brain metabolites (Fig. 5), natural-abundance muscle glycogen (Fig. 6) and ^{13}C-labeled brain glycogen (Fig. 7). In both brain and muscle spectra, the large subcutaneous lipid signal was suppressed by increasing the dynamic range for the smaller signals. The extracerebral lipid signal was suppressed more than 100-fold [19], while some lipid signal remained in muscle spectra (Fig. 6) as expected from the presence of intramyocellular lipids in muscle tissue, as well as interstitial adipose tissue (extramyocellular lipids) [22].

The described sequence allows detection of compounds with very short T_1 and T_2 because the magnetization in the VOI is not manipulated until the 1-D ISIS pulse. This way, relaxation losses are eliminated during OVS which constitutes a significant portion of the time required for localization. By applying 1-D ISIS, the most significant source of contamination, namely, the magnetization between the coil and the VOI, is eliminated, while T_1 relaxation losses due to ISIS are minimized. Note that in phantom experiments much of the localization in the y dimension is achieved by the 1-D ISIS; however in vivo, where motion may reduce ISIS efficiency, OVS in the y dimension improves the localization performance. The time required for localization is only 35 ms (OVS plus ISIS) which does not allow for substantial T_1 recovery of the dephased signal in the outer volume. The OVS uses adiabatic pulses as nominal 90° pulses (in the nonadiabatic mode). With a surface coil these pulses do not result in perfectly homogeneous excitation of the outer volume for

dephasing; however, this can be overcome by minor adjustments to the sequence (Fig. 4c). Namely, with the addition of two low-power OVS pulses at the beginning of the sequence, a better definition of the localized volume can be achieved in three dimensions within the SAR limits set for the brain, which are the most stringent SAR limits for human applications.

With this sequence, we previously detected human brain glycogen after labeling it with [1-^{13}C]glucose [19]. We are currently using this technique routinely in our laboratory to measure human brain glycogen metabolism [23]. An example of brain glycogen quantitation over an extended period of time is shown in Fig. 7. The TRs utilized in these studies (0.3–0.45 s) are 2–3 times the T_1 of glycogen at this magnetic field [5, 6], leading to a high SNR per unit time. A high SNR is also achieved by utilization of a 4 T magnet which is considered currently very high field strength for human applications. With the increasing magnetic field the power requirements increase, making it more difficult to stay within the SAR limits. To accomplish this, pulse shapes and durations were optimized and short acquisition times (25 ms $\sim 3 \cdot T_2^*$) were utilized such that the power deposition due to decoupling was kept small. Additionally, the linear ^{13}C and quadrature ^{1}H coil utilized [11] has reduced power requirements.

In conclusion, content and metabolism of biologically significant compounds with very short T_1 and T_2 relaxation times can be measured efficiently in humans at 4 T by the localized ^{13}C spectroscopy sequence described here.

Acknowledgements

We thank Elizabeth Seaquist, Anjali Kumar, Amy Criego and the nurses and medical assistants of the General Clinical Research Center for their enthusiastic support of the glucose infusion studies, the staff of the Center for MR Research for maintaining and supporting the NMR system, and Pierre-Francois Van De Moortele for expert advice on image analysis.

The Center for MR Research is in part supported by a National Center for Research Resources (NCRR) biotechnology research resource grant P41RR08079 and the General Clinical Research Center at the University of Minnesota by NCRR grant M01RR00400. This research was supported by NIH grant R21 NS45519 from the NINDS and NIDDK (RG) and the Juvenile Diabetes Research Foundation International research grant 1-722-2001 (RG).

References

1. Shulman R.G., Rothman D.L.: Annu. Rev. Physiol. **63**, 15–48 (2001)
2. Gruetter R.: Neurochem. Int. **41**, 143–154 (2002)
3. Ebert D., Haller R.G., Walton M.E.: J. Neurosci. **23**, 5928–5935 (2003)
4. Van Den Bergh A.J., Tack C.J., Van Den Boogert H.J., Vervoort G., Smits P., Heerschap A.: Eur. J. Clin. Invest. **30**, 122–128 (2000)
5. Zang L.H., Laughlin M.R., Rothman D.L., Shulman R.G.: Biochemistry **29**, 6815–6820 (1990)
6. Overloop K., Vanstapel F., Van Hecke P.: Magn. Reson. Med. **36**, 45–51 (1996)

7. Ordidge R.J., Connelly A., Lohman J.A.B.: J. Magn. Reson. **66**, 283–294 (1986)
8. Choi I.Y., Tkáč I., Gruetter R.: Magn. Reson. Med. **44**, 387–394 (2000)
9. Choi I.Y., Tkáč I., Uğurbil K., Gruetter R.: J. Neurochem. **73**, 1300–1308 (1999)
10. Choi I.Y., Wu C., Okar D.A., Lange A.J., Gruetter R.: Eur. J. Biochem. **269**, 4418–4426 (2002)
11. Adriany G., Gruetter R.: J. Magn. Reson. **125**, 178–184 (1997)
12. Gruetter R., Tkáč I.: Magn. Reson. Med. **43**, 319–323 (2000)
13. Gruetter R., Adriany G., Merkle H., Andersen P.M.: Magn. Reson. Med. **36**, 659–664 (1996)
14. Ross B.D., Bluml S., Cowan R., Danielsen E., Farrow N., Gruetter R.: Biophys. Chem. **68**, 161–172 (1997)
15. Gruetter R., Seaquist E.R., Kim S., Uğurbil K.: Dev. Neurosci. **20**, 380–388 (1998)
16. Gruetter R., Uğurbil K., Seaquist E.R.: J. Neurochem. **70**, 397–408 (1998)
17. Seaquist E.R., Gruetter R.: Magn. Reson. Med. **39**, 313–316 (1998)
18. Gruetter R., Seaquist E.R., Uğurbil K.: Am. J. Physiol. Endocrinol. Metab. **281**, E100–112 (2001)
19. Öz G., Henry P.G., Seaquist E.R., Gruetter R.: Neurochem. Int. **43**, 323–329 (2003)
20. Shaka A.J., Keeler J., Freeman R.: J. Magn. Reson. **53**, 313–340 (1983)
21. Carey P.E., Halliday J., Snaar J.E., Morris P.G., Taylor R.: Am. J. Physiol. Endocrinol. Metab. **284**, E688–694 (2003)
22. Boesch C., Kreis R.: Ann. N.Y. Acad. Sci. **904**, 25–31 (2000)
23. Öz G., Lei H., Seaquist E.R., Gruetter R. in: Proceedings of the 12th Scientific Meeting of the International Society for Magnetic Resonance in Medicine, May 15–21, 2004, Kyoto, Japan (Duerk J.Y., ed.), p. 301. Kyoto: ISMRM 2004.

Authors' address: Gülin Öz, Center for Magnetic Resonance Research, Department of Radiology, University of Minnesota, 2021 6th Street SE Minneapolis, MN 55455, USA
E-mail: gulin@cmrr.umn.edu

Verleger: Springer-Verlag GmbH, Sachsenplatz 4–6, 1201 Wien, Österreich. – Herausgeber: Prof. K. M. Salikhov, Zavoisky Physical-Technical Institute, Sibirsky trakt 10/7, 420029 Kazan, Russian Federation. – Hersteller: Satz und Umbruch: Zavoisky Physical-Technical Institute, Sibirsky trakt 10/7, 420029 Kazan, Russian Federation. – Offsetdruck: Druckerei Ferdinand Berger & Söhne GmbH, 3580 Horn, Österreich. – Verlagsort: Wien. – Herstellungsort: Horn. – Printed in Austria.